the FEBS Journal

Human haptoglobin structure and function – a molecular modelling study

F. Polticelli[1], A. Bocedi[1], G. Minervini[1] and P. Ascenzi[1,2]

1 Department of Biology and Interdepartmental Laboratory for Electron Microscopy, University Roma Tre, Italy
2 National Institute for Infectious Diseases I.R.C.C.S. ''Lazzaro Spallanzani'', Rome, Italy

Keywords
chaperone-like activity; covalent multimers; haemoglobin; haptoglobin; homology modelling

Correspondence
F. Polticelli, Department of Biology, University Roma Tre, Viale Guglielmo Marconi 446, I-00146 Rome, Italy
Fax: +39 06 57336321
Tel: +39 06 57336362
E-mail: polticel@uniroma3.it

Database
Models data are available in the Protein Model DataBase under the accession numbers PM0075388 and PM0075389

(Received 8 July 2008, revised 11 September 2008, accepted 17 September 2008)

doi:10.1111/j.1742-4658.2008.06690.x

Hemoglobin is the most prominent protein in blood, transporting O_2 and facilitating reactive oxygen and nitrogen species detoxification. Hemoglobin metabolism leads to the release of extra-erythrocytic hemoglobin, with potentially severe consequences for health. Extra-erythrocytic hemoglobin is complexed to haptoglobin for clearance by tissue macrophages. The human gene for haptoglobin consists of three structural alleles: *Hp1F*, *Hp1S* and *Hp2*. The products of the *Hp1F* and *Hp1S* alleles differ by only one amino acid, whereas the *Hp2* allele is the result of a fusion of the *Hp1F* and *Hp1S* alleles, is present only in humans and gives rise to a longer α-chain. Haptoglobin consists of a dimer of αβ-chains covalently linked by a disulphide bond between the Cys15 residue of each α-chain. However, the presence of the *Hp1* and *Hp2* alleles in humans gives rise to HPT1-1 dimers (covalently linked by Cys15 residues), HPT1-2 hetero-oligomers and HPT2-2 oligomers. In fact, the HPT2 variant displays two free Cys residues (Cys15 and Cys74) whose participation in intermolecular disulphide bonds gives rise to higher-order covalent multimers. Here, the complete modelling of both haptoglobin variants, together with their basic quaternary structure arrangements (i.e. HPT1 dimer and HPT2 trimer), is reported. The structural details of the models, which represent the first complete view of the molecular details of human haptoglobin variants, are discussed in relation to the known haptoglobin function(s).

Hemoglobin (Hb) is the most prominent protein in blood. Hb transports O_2 in the circulatory system and facilitates reactive oxygen and nitrogen species detoxification [1–6]. Hb metabolism leads to the release of the heme protein and of free heme into extracellular fluids, with potentially severe consequences for health [7]. In fact, extra-erythrocytic Hb undergoes renal filtration, leading to renal iron loading if not bound to haptoglobin (HPT) [8]. Hb release into plasma is a physiological phenomenon associated with intravascular hemolysis that occurs during the destruction of senescent erythrocytes and enucleation of erythroblasts [7]. However, intravascular hemolysis becomes a severe pathological complication when it is accelerated in various autoimmune, infectious (such as malaria) and inherited (such as sickle cell disease) disorders [1]. To prevent Hb-mediated pathological events, Hb is complexed to HPT for clearance by tissue macrophages [7]. In parallel to Hb : HPT complex formation, the free heme is scavenged by hemopexin, which delivers it to the liver [7].

HPT, the plasma protein with the highest binding affinity for Hb ($K_d = 10^{-12}$ M), is mainly expressed in the liver and belongs to the family of acute-phase proteins, whose synthesis is induced by several cytokines during the inflammatory processes [9]. HPT is synthesized as a single chain and then cleaved into an N-terminal light α-chain and a C-terminal heavy

Abbreviations
C1R, complement protease C1R; CCP domain, complement control protein domain (also named the Sushi domain); Hb, hemoglobin; HPT, haptoglobin; PDB, Protein Data Bank; SRCR domain, scavenger receptor cysteine-rich domain.

β-chain [10]. The two chains are covalently linked by an intermolecular disulfide bond formed by Cys131 and Cys248 [11]. An Hb dimer binds to the HPT heavy β-chain, and thus the HPT(αβ dimer) : Hb stoichiometry is 1 : 1 [12,13].

In plasma, stable HPT : Hb complexes are formed and subsequently delivered to the reticulo-endothelial system by receptor-mediated endocytosis. CD163, the specific receptor for the HPT : Hb complex [14], is a macrophage-differentiation antigen containing nine copies of the scavenger receptor cysteine-rich (SRCR) domain. Two variants of the SRCR domain proteins (named class A and class B) have been identified in a number of mosaic and transmembrane proteins [15]. CD163 belongs to group B of the SRCR domain proteins, which are characterized by a short cytoplasmic tail, a transmembrane segment and an extracellular region consisting solely of the class B SRCR domains [15,16]. CD163 is exclusively expressed by the monocyte/macrophage lineage and its expression is induced by inflammation [15].

Other than on macrophages, the existence of a receptor for the HPT : Hb complex was demonstrated also on hepatocytes and hepatoma cell lines. After internalization into the liver parenchymal cells, organelles containing the HPT : Hb complex distribute in the microsome fraction where the complex dissociates and the subunits are subsequently degraded [17–21].

The human gene for HPT, located on chromosome 16q22, consists of three structural alleles: *Hp1F*, *Hp1S* and *Hp2* [22,23]. The products of the *Hp1F* and *Hp1S* alleles differ by only one amino acid: Lys54 of the Hp1S-chain is replaced by Glu in the Hp1F-chain [22]. The *Hp2* allele, which probably originated by a nonhomologous crossing-over event, is the result of a fusion of the *Hp1F* and *Hp1S* alleles, and is present only in humans [22,23], although similar but independent events have been very recently evidenced in other mammals such as deer and cow [24,25]. The human *Hp2* allele gives rise to a longer chain (388 amino acids as opposed to 329 in the chains originating from the *Hp1* alleles). The heavy β-chain of HPT displays a fairly high homology to the catalytic domain of serine proteases, although the residues His and Ser, participating in the catalytic triad, are not conserved [26] (Fig. 1). On the other hand, it is interesting to note the conservation of Asp193, orthologous to Asp194 of serine proteases, which is involved in the conformational

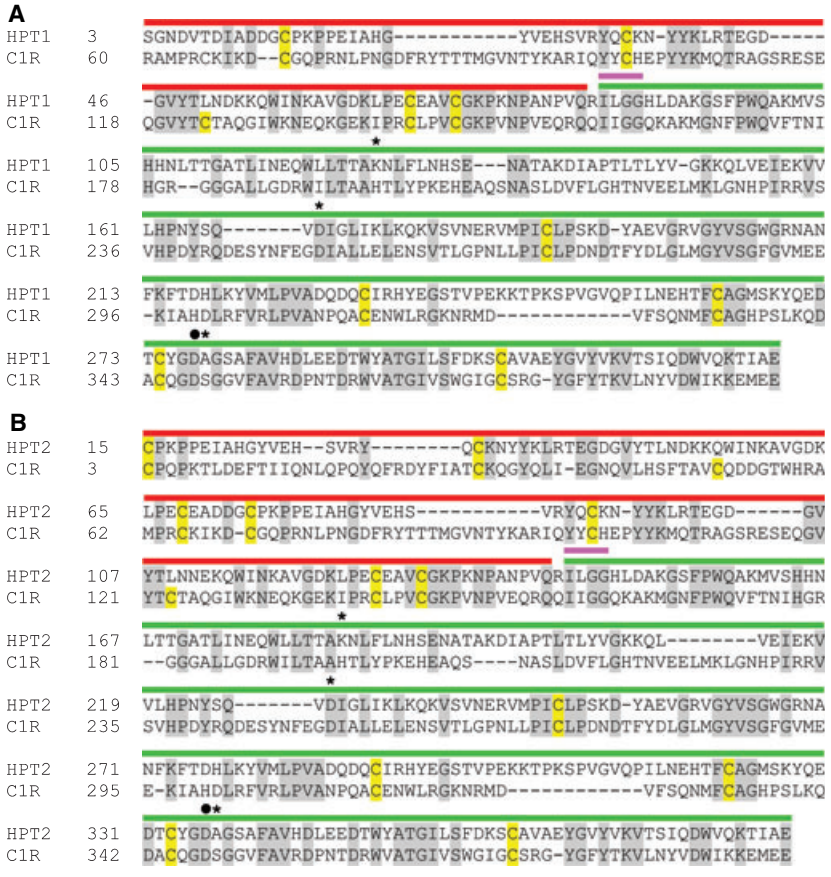

Fig. 1. Amino acid sequence alignment between HPT1 and C1R (A), and between HPT2 and C1R (B). Conserved residues are shaded in grey; Cys residues are highlighted in yellow. Above the sequence alignment, red, green and magenta bars indicate α- and β-chains, and the Ile1–Leu2–Gly3–Gly4 N-terminal sequence, respectively; stars indicate residues orthologous to those of the serine proteases catalytic triad; and the black circle indicates Asp193, orthologous to the trypsin-like serine (pro)enzymes Asp194.

change(s) taking place following proteolytic activation of the zymogen, forming a salt bridge with the N-terminal charged amino group. Remarkably, the homology with trypsin-like enzymes extends also to the N-terminal dipeptide (Ile1–Leu2 in HPT and Ile1–Val2/Leu2/Ile2 in trypsin-like enzymes) and to the Gly3–Gly4 hinge region [26] (Fig. 1). The quaternary structure of HPT in organisms other than humans consists of a dimer of αβ-chains covalently linked by a disulphide bond between the Cys15 residue of each α-chain. However, in humans the presence of the *Hp1* and *Hp2* alleles gives rise to HPT1-1 dimers (covalently linked by Cys15 residues), HPT1-2 hetero-oligomers and HPT2-2 oligomers [11,22]. In fact, by the effect of partial fusion of *Hp1F* and *Hp1S* alleles, the HPT2 variant displays two free Cys residues (Cys15 and Cys74), whose participation in intermolecular disulphide bonds gives rise to higher-order covalent multimers [11].

Data regarding the molecular details of monomeric HPT1 and HPT2 variants and oligomers are very scarce. No 3D structure is available for any of the human HPT variants, except for a molecular model of the HPT1 variant built using a composite template based on the homology between the HPT β-chain and the serine protease fold, and the homology between the HPT1 α-chain and the complement control proteins (CCP), or Sushi domain, of complement C1S protease [26]. Additional data regarding the quaternary structure of HPT variants are essentially those deriving from a dated, albeit very careful, electron microscopy analysis of both the Hb-free and Hb-bound HPT1 and HPT2 variants [11,13]. In this latter study it has been evidenced that HPT1 forms covalent dimers made up of two αβ-chains, while HPT2 forms covalent trimers and higher-order oligomers of αβ-chains [11].

Recently, the crystal structure of the full-length zymogen catalytic domain of the complement protease C1R (C1R) has been determined [27]. This protein displays a fairly high sequence identity to both HPT variants (approximately 29%; Fig. 1) spanning the entire length of both α- and β-chains. The availability of a template that spans the entire length of both HPT variants and provides the likely relative arrangement of the two HPT chains prompted us to carry out complete modelling of both HPT variants together with their basic quaternary structures (i.e. HPT1 dimer and HPT2 trimer). The structural details of the models, which represent the first complete view of the molecular details of human HPT variants, are discussed in relation to the HPT physiological function(s).

Results and Discussion

Modelling of the αβ 'monomers' of HPT1 and HPT2

Figure 1 shows the sequence alignment of the two HPT variants and C1R. C1R displays 29% sequence identity to both HPT1 (spanning residues 15–328, covering both the HPT1 α- and β-chains) and HPT2 (spanning residues 15–387, covering both HPT2 α- and β-chains) variants. The homology is widespread along all the sequences, and almost all the Cys residues involved in disulphide bonds in C1R are conserved in both HPT variants. In detail, 14 Cys residues are present in C1R, all of which are involved in disulphide bonds (the Cys pairing being: 3–52, 32–65, 70–123, 100–141, 145–271, 314–333 and 344–374, numbered according to the C1R crystal structure; protein data bank (PDB) code: 1GPZ [27]). The Cys residue orthologous to C1R Cys123 is substituted by Leu in HPT1 (Fig. 1A) and Cys residues orthologous to C1R Cys52 and Cys123 are substituted by Gln and Leu, respectively in HPT2 (Fig. 1B). The result of these substitutions is that HPT1 Cys15 and HPT2 Cys15 and Cys74 are predicted not to be involved in disulphide bonds, as indeed has been demonstrated experimentally [28], whereas all other disulfide bonds are conserved in both HPT variants.

The modelled 3D structures of HPT1 and HPT2 αβ 'monomers' are shown in Fig. 2. Cys15 is located on the tip of the N-terminal CCP domain in both HPT1

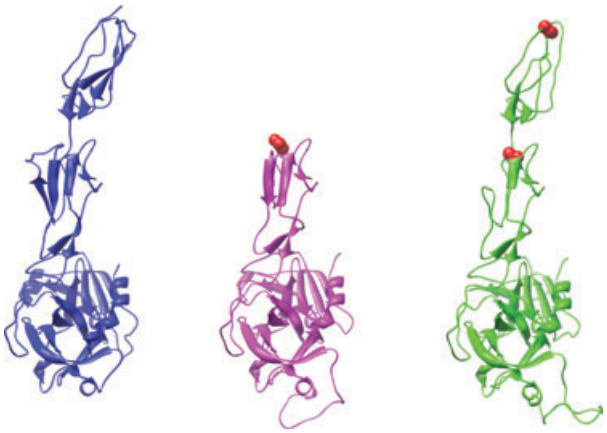

Fig. 2. Schematic representation of the 3D structure of C1R (PDB code: 1GPZ [27]) and of the modelled structures of HPT1 and HPT2. HPT1 residue Cys15 and HPT2 residues Cys15 and Cys74 are shown in spacefill representation. This and the following figures were produced using CHIMERA [43].

and HPT2, whereas Cys74 is located in the region connecting the two CCP modules in HPT2, where the low steric hindrance allows the formation of intermolecular disulphide bonds (Fig. 2).

CD spectroscopy data, available only for the HPT1 variant [26], indicate an α-helix content ranging from 3.6 to 9.9% and a β-sheet content ranging from 32.9 to 40.9%. The HPT1 model presented here displays 9.5% α-helix content and 28.6% β-sheet content, which is in fairly good agreement with the experimental data. In addition, both models display a good stereochemical quality, as evaluated using PROCHECK [29]. In fact, G-values calculated using PROCHECK were −0.20 and −0.24 for HPT1 and HPT2, respectively, well above the threshold of −0.5 for good quality models, and approximately 97% of residues in both models were observed to lie in the allowed regions of the Ramachandran plot. It is interesting to note that the secondary structure content of the two CCP modules of HPT2 was lower than that of the single CCP module of HPT1. This could be a result of the fact that the full-length zymogen catalytic domain of the complement protease C1R is a better template for HPT1 than for HPT2 in the CCP modules protein region. In fact, considering only this region, HPT1 displays 31% identity with C1R, whereas HPT2 displays 25% identity.

The HPT1 model shown in Fig. 2 differs from that reported by Ettrich and coworkers [26] in the location of the Cys15 residue. In the model reported by Ettrich and coworkers [26], Cys15 appears to be located in the middle of the β strands of the CCP module, near the region connecting the α and β HPT1 chains, whereas in the models presented here Cys15 is located on the tip of the N-terminal CCP domain. This latter location is consistent with the low steric hindrance required for the formation of inter-chain disulphide bonds in HPT1 and with the location of the orthologous Cys residue found in C1S (PDB code: 1ELV [30]). Furthermore, the terminal location of Cys15 in both HPT variants results in HPT1 covalent dimers and HPT2 covalent trimers whose dimensions are in very good agreement with those obtained by electron microscopy measurements (see below) [11,13].

Modelling of the quaternary structure of HPT1 and HPT2

Based on the electron microscopy data [11,13], the HPT1 quaternary structure consists of a dimer covalently linked by a disulphide bond between Cys15 residues of each α-chain. Accordingly, the molecular model of dimeric HPT1 is formed through a tip-to-tip arrangement of two αβ 'monomers', giving rise to a bilobated structure in which the two heavy β-chains are separated by two α-chains in a linear arrangement (Fig. 3). The minimum and maximum distance between the two heavy β-chains in the modelled HPT1 dimer are approximately 60 and 130 Å, respectively, which compare quite well with distances obtained by electron microscopy measurements (50 and 124 Å, respectively [13]). Moreover, the heavy β-chain diameter determined here is approximately 35 Å compared with the value of 37 Å measured by electron microscopy [13].

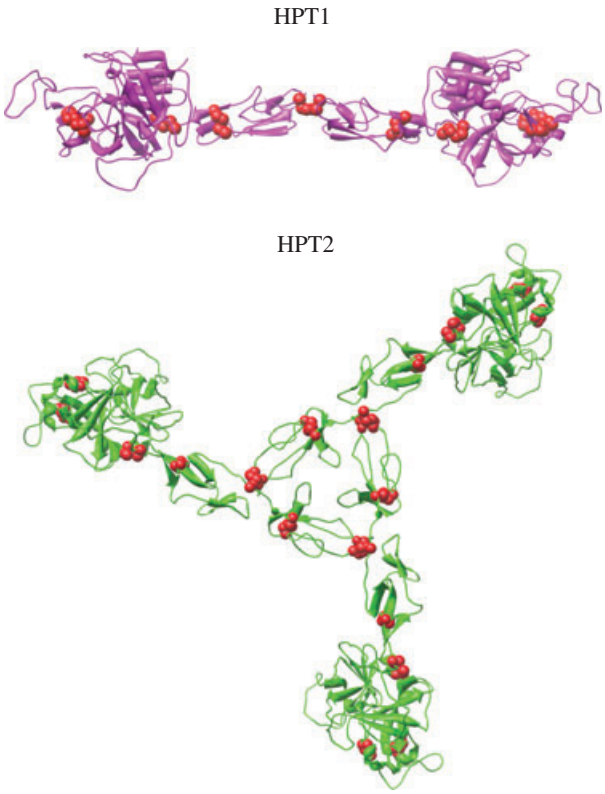

Fig. 3. Quaternary structure model of dimeric HPT1 and trimeric HPT2. Interchain disulphide bonds are shown in spacefill representation.

At variance with dimeric HPT1, the HPT2 variant forms higher-order multimers, the minimum number of subunits involved being three [11,22]. The simplest 'closed symmetric' arrangement of HPT2 αβ 'monomers' that can give rise to covalently linked HPT2 trimers is the one shown in Fig. 3B, in which Cys15 of each monomer forms a disulphide bond with Cys74 of a neighbour monomer. The modelled trimer is fully compatible with both the symmetric arrangement of the heavy β-chains and the formation of a triangle-shaped connecting region observed in electron microscopy studies [11]. In addition, the center-to-center distance between two heavy β-chains in the modelled

HPT2 trimer is approximately 120 Å, a value which compares well with that estimated by electron microscopy (approximately 129 Å) [11].

An interesting feature of the 'closed symmetrical' modelled trimer, which sheds light on the possible mechanism of formation of HPT2 trimeric species, is the presence of several intermolecular electrostatic interactions taking place at the interface between the tip of the N-terminal CCP module of one αβ 'monomer' (where Cys15 is located) and the region connecting the two CCP modules of another αβ 'monomer' (where Cys74 is located). In detail, positively charged Lys17 and Lys64 of one monomer are located in the vicinity of negatively charged Glu79 and Asp45, respectively, of a second monomer (Fig. 4). These residues provide a sort of 'electrostatic docking' site, which can facilitate the proper relative orientation of two monomers to form the Cys15–Cys74 disulphide bond and give rise to trimers, tetramers and higher-order multimers (Fig. 5).

Hb binding and chaperone-like activity of HPT

Selective proteolysis studies have demonstrated that the Hb-binding site lies in the region surrounding residues 9 and 10, and the 128–137 loop of the HPT β-chain, while the HPT α-chain is not involved in Hb binding [31]. In agreement, in our model the β-chain N-terminal residues partially overlap with the 128–137 loop region (Fig. 6). An interesting feature of the HPT β-chain is that its N-terminus is highly homologous to

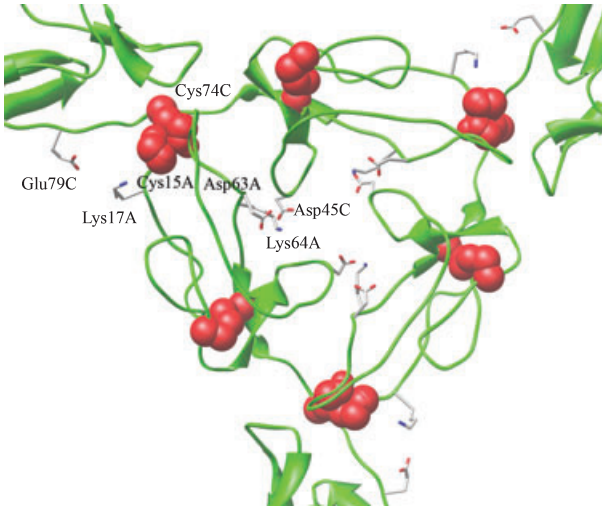

Fig. 4. Schematic representation of the electrostatic interactions taking place between HPT2 monomers at the closed trimer interface. For clarity only residues at the interface between monomers A and C are labeled. Interchain disulphide bonds are shown in spacefill representation.

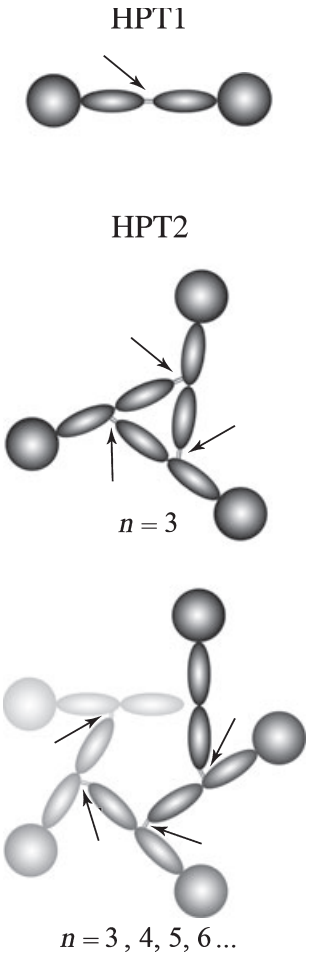

Fig. 5. Schematic representation of the main quaternary structure arrangements of HPT1 and HPT2. The spheres represent HPT β-chains while ellipses represent the CCP modules of HPT α-chains. Intermolecular disulphide bonds are represented by double lines and indicated by arrows. The bottom panel highlights the fact that HPT2 exists also in oligomerization states larger than 3 that can give rise to both closed (no free Cys residues) and opened (free Cys residues) oligomers.

that of serine proteases [26] and that residue Asp194, which in the latter class of enzymes binds the N-terminal ammonium group following proteolytic activation of the zymogen, is conserved in HPT as Asp193. Thus, it is probable that also in HPT the N-terminal region binds in the protein cavity on the bottom of which Asp193 lies, thus leading to structuring of this protein region to form the Hb-binding site (see below).

A large hydrophobic region is adjacent to the Hb-binding site (Fig. 6). This region, the largest hydrophobic solvent-exposed area on the HPT β-chain, has been hypothesized to be responsible for the chaperone-like activity of HPT [26], the property of HPT to prevent thermally induced aggregation of proteins

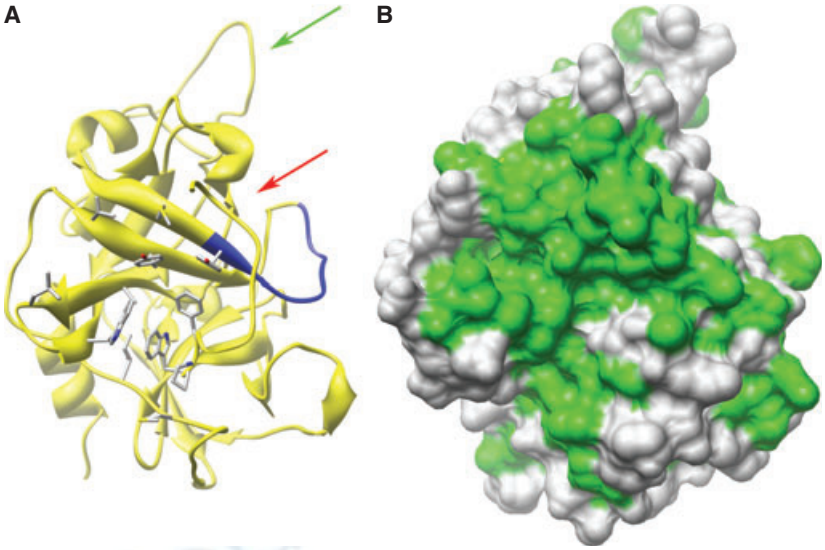

Fig. 6. Schematic representation of the 3D structure of the HPT β-chain (A). The 128–137 residue region, involved in Hb binding, is coloured in blue. Residues building up the adjacent large hydrophobic region are shown in stick representation. The red arrow indicates the cavity on the bottom of which Asp193 is located. The green arrow indicates the CD163-binding loop. Panel B shows the molecular surface of the HPT β-chain shown in the same orientation as panel A. Surface areas generated by hydrophobic and polar residues are coloured in green and grey, respectively.

[26,32]. Titration experiments have also demonstrated that the chaperone-like activity of HPT decreases by up to 50% upon addition of Hb, until a 1 : 1 HPT : Hb ratio is reached [26]. Our model is consistent with these data, in that binding of the Hb αβ-dimer (approximately 50 Å in diameter) to the 128–137 loop region of HPT would, at least partially, cover up the solvent-exposed hydrophobic surface of HPT.

The comparative analysis of the primary and tertiary structures of trypsin-like serine proteases and HPT suggests that HPT chaperone-like activity may be modulated by the formation of the intramolecular salt bridge between the Ile1 N-terminus and Asp193. Note that the endogenous and exogenous Ile–Leu-like dipeptides have been demonstrated to activate trypsinogen by forming a salt bridge with the Asp194 residue [33,34], hortologous to HPT Asp193. Interestingly, the pH-dependent chaperone-like activity of HPT increases with pH in the range 5.5–7.5 with an apparent pK $\sim$ 6.5 [32]. To test the hypothesis that HPT activation could be related to binding of the Ile1–Leu2 N-terminal tail to Asp193, the pK_a values of HPT β-chain and trypsinogen-ionizable residues were calculated using the PROPKA software [35]. The HPT Asp193 pK_a value was 6.2; this value correlates well with the experimentally determined midpoint of the pH dependence of HPT chaperone-like activity ($\sim$ 6.5). Interestingly, the calculated pK_a value of trypsinogen Asp194 resulted to be 6.2 as well.

The CD163-binding region

Recently, using recombinant HPT/HPT-related protein chimeras complexed to Hb, it has been shown that only the HPT β-chain is involved in binding of the HPT : Hb complex by the CD163 receptor [36]. In particular, the loop encompassing residues Val157–Thr162 of the HPT β-chain has been demonstrated to be essential for receptor binding [36]. The 157–162 loop is located near the Hb-binding loop in our HPT model (Fig. 6), in agreement with the observation that the epitope recognized by CD163 is formed by residues contributed by both HPT and Hb. In fact, CD163 binds the HPT : Hb complex with an affinity at least two orders of magnitude higher than HPT and Hb alone [36].

Conclusions

The best-characterized function of HPT is that of binding free Hb and promoting its endocytosis and subsequent intracellular degradation through the formation of high-affinity complexes with the CD163 scavenger receptor on macrophages. In this way HPT reduces the loss of free Hb through glomerular filtration and promotes the recycling of iron. In addition, heme and iron released from free Hb generate reactive oxygen species leading to tissue injury, as demonstrated *in vivo* in HPT knockout mice. Thus, HPT, promoting immediate clearance of free Hb, acts as an antioxidant agent [37].

An additional activity of HPT is related to its ability to suppress heat-induced and oxidative stress-induced unfolding and precipitation of a number of proteins, thus reducing the toxic effects caused by aggregation of misfolded extracellular proteins. Taken together, these findings indicate that HPT plays a significant role in re-establishing homeostasis after local or systemic

infection by virtue of its various anti-inflammatory activities [32].

Particularly intriguing is the hypothesis that HPT may undergo a conformational re-arrangement following proteolytic maturation of the protein, similarly to the proteolytic activation mechanism observed in serine proteases. The structural model presented in this work supports this hypothesis. In fact, binding of the Ile1–Leu2 N-terminal tail of the HPT β-chain to the Asp193 pocket would lead to a structural re-arrangement of both the Hb-binding region and of the adjacent hydrophobic surface area available for binding misfolded proteins. In addition, pK_a calculations indicate that Asp193, as a result of its poorly solvent-accessible location on the HPT surface, is characterized by an altered pK_a value (= 6.2) which correlates well with the pH dependence of the chaperone-like activity of HPT (midpoint $\sim$ 6.5 [32]). This could easily be explained by the ability of Asp193 to drive the conformational rearrangement of HPT only in the deprotonated form, with the ability to form a salt bridge with the N-terminal ammonium group of the protein, as reported for serine (pro)enzyme activation [33,34]. The common architecture of the HPT β-chain and of trypsin-like (pro)enzymes, together with similar structural and electrostatic properties at the root of the activation mechanism, may represent a case of divergent evolution. Indeed, the HPT β-chain appears to have evolved from a common ancestor by mutation of only two out of three catalytic residues (His $\rightarrow$ Lys and Ser $\rightarrow$ Ala) while preserving the overall fold and probably the activation mechanism [26,33,34].

In conclusion, in this work we present the first complete description of the molecular details of HPT1 and HPT2 monomers and multimers and show that the information deriving from the calculated models can be useful to explain some of the properties of the multifunctional human HPT variants.

Materials and methods

The molecular models of HPT1 and HPT2 were built using the crystal structure of C1R as the template (PDB code: 1GPZ [27]). In detail, protein sequences displaying significant similarity with HPT variants were retrieved through three PSI-BLAST [38] iterations against the nonredundant protein database using the sequences coded GI 1212947 and GI 4826762 for HPT1 and HPT2 variants, respectively, as a bait. The 18 N-terminal amino acids of both HPT1 and HPT2 sequences, which represent a signal peptide, were previously removed. PSI-BLAST E-values of C1R were 2×10^{-109} and 1×10^{-126} for HPT1 and HPT2 variants, respectively. Amino acid sequence alignment between the template C1R and the two HPT variants was then obtained through multiple sequence alignment of the PSI-BLAST hits using CLUSTALW [39]. This procedure yielded the alignments shown in Fig. 1.

The molecular models of the two HPT1 and HPT2 variants were built using the program NEST [40], a fast model-building program that applies an 'artificial evolution' algorithm to construct a model from a given template and alignment. The NEST option *tune 2* was used to refine the alignment, avoiding the unlikely occurrence of insertions and deletions within template secondary-structure elements.

The HPT1 covalent dimer and the HPT2 covalent trimer were constructed using the molecular graphics package Discovery Studio VISUALIZER 1.7 (Accelrys Software Inc., San Diego, CA, USA) and the rototranslation matrices given in Table S1. Constraints considered for HPT1 dimer construction were its binary symmetry and the formation of the Cys15–Cys15 intermolecular disulphide bond [11,13]. Analogously, constraints used for HPT2-2 trimer construction were its ternary symmetry and the formation of the Cys15–Cys74 intermolecular disulphide bonds [11,13].

Monomer and multimer models obtained using the above-described procedure were stereochemically regularized through energy minimization using the CHARMM macromolecular mechanics package [41], c33b1 version, and the CHARMM27 parameters and force field [42]. The stereochemical quality of the models was evaluated using PROCHECK [29].

The molecular surface of the HPT β-chain was calculated and visualized using the program CHIMERA [43]. The HPT β-chain and bovine trypsinogen (PDB code 1TGN [44]) ionizable residue pK_a values were calculated using PROPKA [35].

Acknowledgements

This work was supported by a grant from the Italian Ministry of University and Research.

References

1 Bunn HF & Forget BG (1986) *Hemoglobin: Molecular, Genetic and Clinical Aspects*. Saunders, Philadelphia, PA.
2 Perutz MF (1990) Mechanisms regulating the reactions of human hemoglobin with oxygen and carbon monoxide. *Annu Rev Physiol* **52**, 1–25.
3 Brunori M (1999) Hemoglobin is an honorary enzyme. *Trends Biochem Sci* **24**, 158–161.
4 Gow AJ, Luchsinger BP, Pawloski JR, Singel DJ & Stamler JS (1999) The oxyhemoglobin reaction of nitric oxide. *Proc Natl Acad Sci USA* **96**, 9027–9032.
5 Imai K (1999) The hemoglobin enzyme. *Nature* **401**, 437–439.